Conjugates between minor groove binders and Zn(II)-tach complexes: Synthesis, characterization, and interaction with plasmid DNA

Claudia Sissi [a, **], Luca Dovigo [a], Maria Laura Greco [a], Antonella Ciancetta [b], Stefano Moro [b, ***], Jakub W. Trzciński [c], Fabrizio Mancin [c], Paola Rossi [d], Giampiero Spalluto [d, ****], Paolo Tecilla [d, *]

[a] Department of Pharmaceutical and Pharmacological Sciences, University of Padova, Via Marzolo 5, Padova, Italy
[b] Molecular Modeling Section (MMS), Department of Pharmaceutical and Pharmacological Sciences, University of Padova, Via Marzolo 5, Padova, Italy
[c] Department of Chemical Sciences, University of Padova, Via Marzolo 1, Padova, Italy
[d] Department of Chemical and Pharmaceutical Sciences, University of Trieste, Via Giorgieri 1, Trieste, Italy

ARTICLE INFO

Article history:
Received 27 December 2016
Received in revised form
28 March 2017
Accepted 10 April 2017
Available online 11 April 2017

Keywords:
Synthetic nuclease
DNA
Minor groove binder
Tach
Zn(II) complexes

ABSTRACT

A new family of conjugates between a Zn(II)-tach complex and $(indole)_2$ or benzofuran-indole amide minor groove binders connected through alkyl or oxyethyl linkers of different lengths has been prepared. The conjugates bind strongly to DNA. However, the complexation to DNA to promote the Zn(II) catalyzed hydrolytic cleavage of the DNA results instead in its inhibition. This inhibition effect has been confirmed also using Cu(II). Modeling studies suggest that in the most stable complex conformation, the minor groove binder and the linker lie in the minor groove hampering the interaction between the metal complex and the phosphate backbone of DNA. Therefore, the linear arrangement of minor groove binder-linker-metal complex appears to be effective to ensure tight binding but unproductive from a hydrolytic point of view.

1. Introduction

The first report of a metal ion complex able to hydrolytically cleave DNA was published more than 25 years ago.[1] Nevertheless, the interest in synthetic DNA hydrolytic agents based on metal complexes is still increasing due to the promising applications of such systems in DNA manipulation, a key tool in the field of biotechnology.[2] On the other hand, some issues about activity and sequence selectivity are still partly unresolved. Indeed, with the notable exception of Ce(IV) based catalysts,[3] many of the reported cleavage agents show moderate activity at low concentration and/or scarce sequence selectivity. Moreover, many complexes are based on metal ions such as Cu(II),[4] in which oxidative cleavage often competes with the desired hydrolysis of DNA. The use of intrinsically less reactive but hydrolytically more stable ions such as Zn(II)[5] has been less investigated. In recent years, several approaches have been exploited in order to develop more potent and selective artificial nucleases. As an example, di-metallic or poly-metallic complexes have been used in order to increase the catalytic activity.[6,7] Alternatively, conjugation of the metal complexes with DNA binders has been considered to promote interaction of the cleaving agents with the substrate. This last approach is particularly interesting because a tailored DNA binder may contemporaneously ensure high affinity and sequence selectivity. Following this rationale, several systems have been reported in which the hydrolytically active metal ion complex is conjugated to base pairs intercalators,[8–12] major groove binders,[13] nucleobases,[14,15] DNA or PNA fragments,[16,17] simple positively charged group,[18,19] etc. In general, but not always, the increased affinity of the conjugate for the substrate ensures higher activity with respect to the isolated metal complex. These studies pointed out the importance of a correct design because, for example, factors such as the incorrect length of the linker between the metal complex and the DNA binder may lead to unaltered or even decreased reactivity.[8,9]

Among the different types of DNA ligands, minor groove binders

* Corresponding author.
** Corresponding author.
*** Corresponding author.
**** Corresponding author.
E-mail address: ptecilla@units.it (P. Tecilla).

http://dx.doi.org/10.1016/j.tet.2017.04.013

appear quite interesting because they bind tightly to DNA with some sequence selectivity. Pioneering work of Dervan on *N*-methylpyrrole/N-methylimidazole polyamides (Py/Im) has shown that these ligands bind strongly to the minor groove of DNA selectively recognizing C-G rich sequences.[20] This sequence selectivity can be modulated by changing the structure of the ligand and Im/Py and Py/Py polyamides target G-C and A-T (or T-A) rich sequences, respectively.[21] Moreover, work from the group of Boger has demonstrated that minor groove binders based on oligoindole polyamides ensure high DNA affinity and T-A sequence selectivity.[22] Conjugation of oxidative metal complexes[23] or of alkylating reactive centers[24] to such minor groove ligands led to synthetic agents able to damage DNA with high potency and sequence selectivity. Somewhat surprisingly, this approach has been almost overlooked in the design of hydrolytic synthetic nucleases and the examples reported in the literature are very rare. The group of Qiao and Zhao, has reported a mononuclear Zn(II) complex appended to Py-based oligopolyamides of different length which, although at high concentration, showed enhanced reactivity respect to the Zn(II) complex alone and some selectivity toward A-T rich sequences.[25] More recently the same group has described a conjugate between the same minor groove ligand and a bi-metallic Zn(II) complex which shows a marked preference for double strand with respect to random single strand cleavage. This is a consequence of the tight binding to DNA which fixes the hydrolytic catalyst in a certain site increasing the probability of double strand cleavage.[26]

On this premise and following our interest in the design of synthetic nucleases,[27] we decided to explore further the potential of minor groove ligands as elements to improve activity and selectivity of the hydrolytic catalyst. As a DNA ligand we chose the $(indole)_2$ or benzofuran-indole amides which were appended to a Zn(II)-triaminocyclohexane complex using flexible linkers of different length and nature. Here we report the synthesis, characterization and DNA interaction studies of this new class of compound. Somehow disappointingly our compounds bind tightly to DNA but they are inactive in its cleavage. An interpretation of this behavior based on molecular modeling studies will be presented.

2. Result and discussion

2.1. Design and synthesis of the minor groove binder tach conjugates

The structures of the minor groove binder/tach conjugates investigated in this work are reported in Fig. 1. The DNA ligand is in each case an $(indole)_2$ amide except in compound **5** which features a benzofuran-indole amide. These ligands have been chosen because they combine relatively simple synthetic accessibility with a tight binding in the DNA minor groove with sequence selectivity for A-T rich regions. Moreover, studies on duocarmycin models in which the DNA ligand portion have been systematically varied have shown that an indole dimeric structure is long enough to maintain the binding and DNA damaging ability of the native drug thus avoiding the need for the synthesis of longer polyamides.[22,24] The *cis,cis*-triaminocyclohexane (tach) metal ion chelating subunit was chosen on the basis of our previous studies which have shown that its Zn(II) complex is a rather efficient catalyst for the cleavage of model phosphate esters and plasmid DNA.[8] The DNA binder and the catalytic subunits were connected through a flexible linker of different length and polarity with the aim to get insight into the role played by the linker length and nature in determining the reactivity of the systems. Finally compound **8** was designed with a hairpin structure that should ensure a correct and more fixed positioning of the tach-Zn(II) complex in the proximity of the phosphate backbone of DNA.

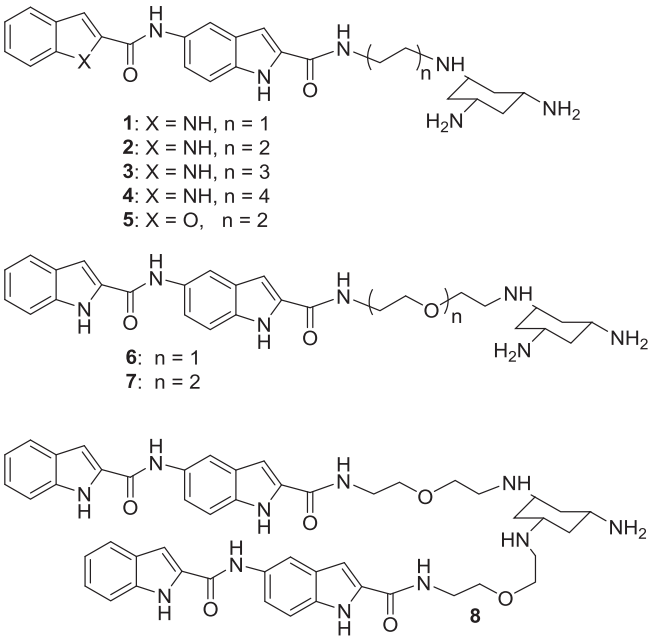

Fig. 1. Structures of the minor groove binder tach conjugates prepared.

The general synthetic route for the synthesis of the conjugates **1**–**7** is shown in Scheme 1. Appropriate amine counterparts **9**–**14**,

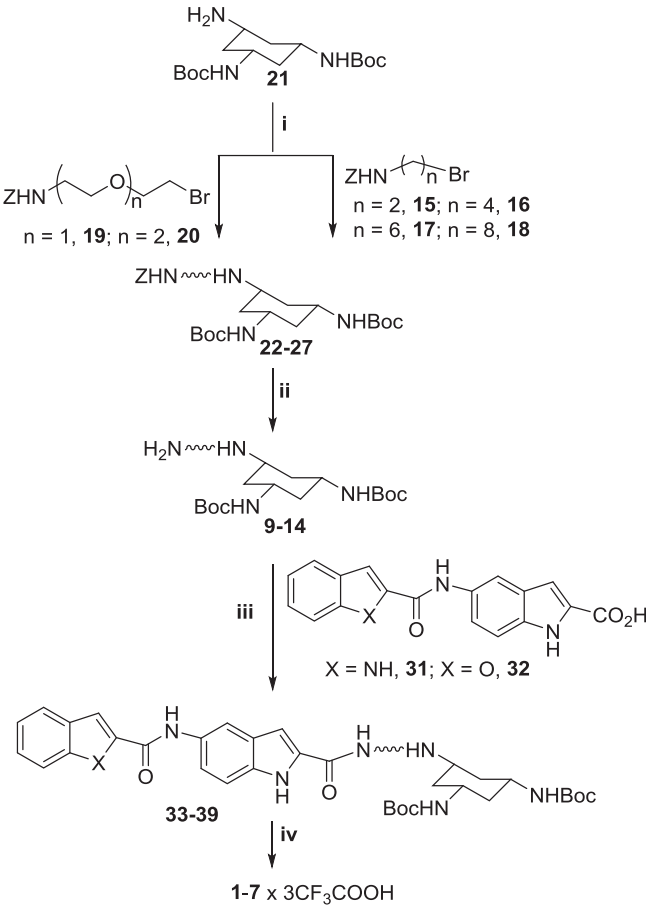

Scheme 1. Reagents: **i**: CH_3CN, DIPEA, reflux; **ii**: CH_3OH, H_2, Pd–C 10%, **iii**: DMF, EDC, Et_3N, rt 72 h; **iv**: CH_2Cl_2-TFA 1:1, rt 4 h.

were obtained by alkylation with bromoalkyl(oxy)amines **15**–**20**, protected at the amino functions as benzyloxycarbonyl derivatives, of tach di-Boc (**21**), in the presence of DIPEA at reflux to give compounds **22**–**27**, as previously reported.[8] Then, treatment of compounds **22**–**27**, with hydrogen in the presence of Pd–C afforded the desired amine derivatives **9**–**14**. Compounds **1**–**7** were easily obtained as trifluoroacetate salts by coupling amino derivatives **9**–**14** with the bis-indole (**31**) or benzofuran-indole (**32**) carboxylic acids[28] in the presence of EDC at room temperature to afford amido compounds **33**–**39**, followed by deprotection at the amino functions by treatment with TFA in CH_2Cl_2 at room temperature.

The synthesis of the hairpin derivative **8** follows similar procedures and is shown in Scheme 2. The mono-BOC-protected derivative of the triaminocyclohexane (**28**) was reacted with two equivalents of **19** affording the corresponding bis-alkylated derivative **29**, that after hydrogenolysis gave the desired amino compound **30**. This latter was coupled with **31** in the presence of EDC affording derivative **40** which after *N*-Boc deprotection with TFA gave final compound **8** as the trifluoroacetate salt.

The Zn(II) and Cu(II) complexes of the tach conjugates were finally prepared following a simple procedure previously optimized by us.[8] In this method the complexes are directly prepared by addition of one equivalent of $Zn(NO_3)_2$ or $Cu(NO_3)_2$ water solution to millimolar solutions of the ligands in water/MeOH mixtures and by adjusting the final pH to 7.0 with NaOH (Scheme 3). The solution obtained is then directly used as the mother solution in the studies with DNA.

The formation of the metal complexes was confirmed by ESI-MS and Fig. 2 reports as a representative example the results obtained with compound **4**. The mass spectra show the formation of the (**4**-H^+)·Zn(II) and (**4**-H^+)·Cu(II) complex at m/z = 620.2 and 619.2, respectively. The small peak at m/z = 558.3, visible in the spectra, is the residual free ligand. The insets of Fig. 2 show the calculated isotopic cluster distributions which match very well the experimentally observed distributions for the two metal complexes. The

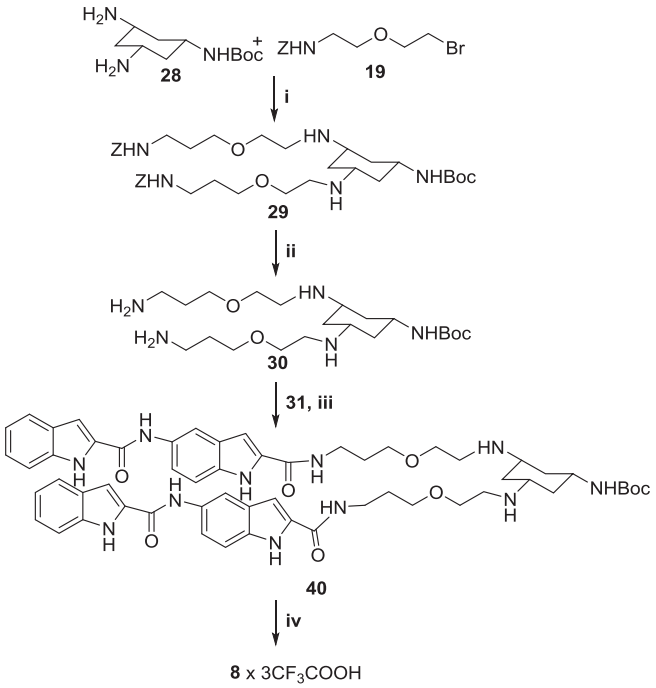

Scheme 2. Reagents: **i**: CH_3CN, DPEA, reflux; **ii**: CH_3OH, H_2, C–Pd 10%; **iii**: DMF, EDC, Et_3N, rt 72 h; **iv**: CH_2Cl_2-TFA 1:1, rt 4 h.

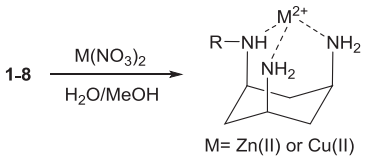

Scheme 3. Formation of the metal complexes of compounds **1**–**8**.

peak at m/z = 652.3 observed in the case of Zn(II) is attributed to a dimeric structure with two methoxides bridging the two metal ions.

2.2. Interaction of the tach conjugates with DNA

The ability of the Zn(II) complexes of the tach-DNA minor groove binder conjugates to bind DNA was preliminarily and qualitatively evaluated by electrophoretic measurements. Increasing amounts of the tested Zn(II) complexes were added to a solution of pBR332 plasmid DNA in HEPES buffer at pH 7.1. After mixing, the solutions were immediately loaded on an agarose gel without any incubation time. Fig. 3 shows the results obtained with

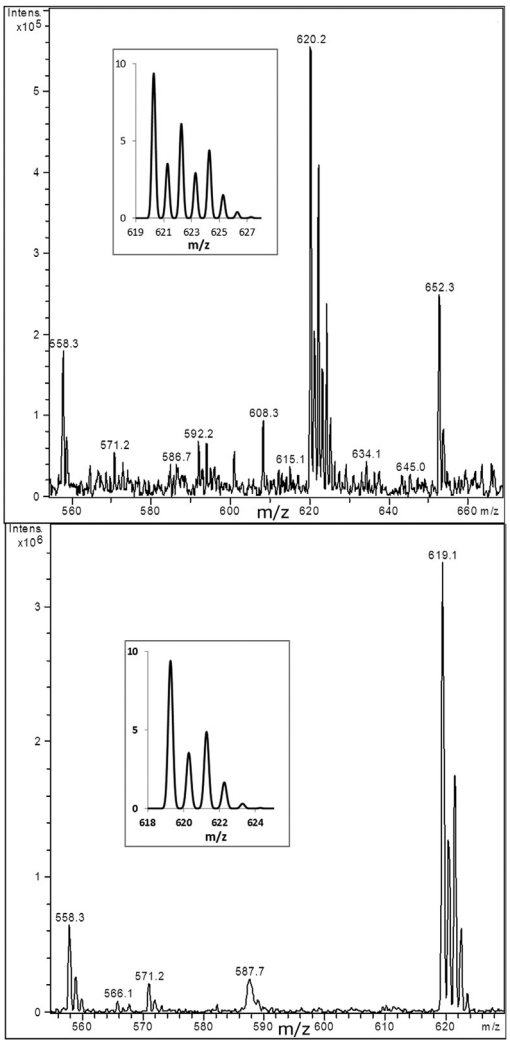

Fig. 2. ESI-MS spectra of the complexes between compound **4** and $Zn(NO_3)_2$ (top) and $Cu(NO_3)_2$ (bottom). The inset shows the calculated isotopic cluster distributions for the complexes with formula (4-H^+)·Zn(II) (top) and (**4**-H^+)·Cu(II) (bottom).

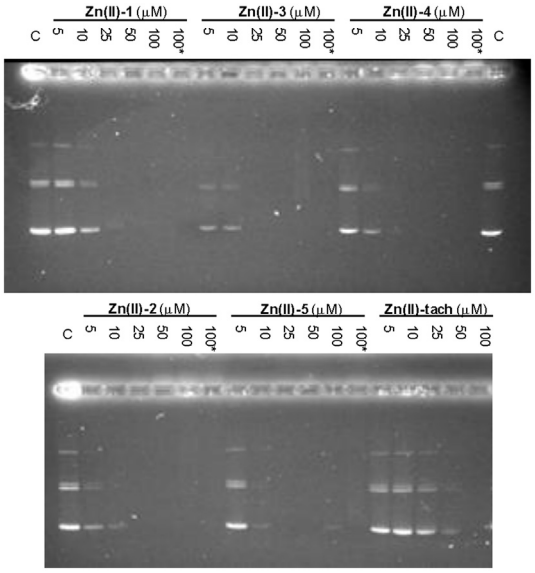

Fig. 3. Agarose gel electrophoresis of pBR322 DNA (12 μM) in the presence of the indicated concentration of the Zn(II) complexes of ligands **1**–**5** and tach in 20 mM HEPES, pH 7.1, 37 °C. Lane* are the ligands in the absence of metal ion. Lane C is the DNA control in the absence of additives. The gel has been loaded immediately after preparation of the different solution without incubation time.

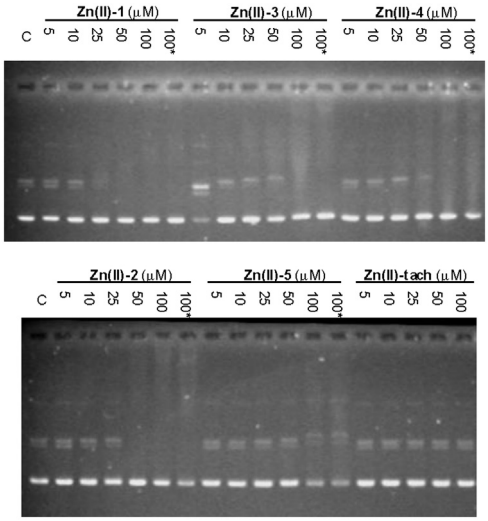

Fig. 4. Agarose gel electrophoresis of pBR322 DNA (12 μM) in the presence of the indicated concentration of the Zn(II) complexes of ligands **1**–**5** and tach in 20 mM HEPES containing EDTA and SDS, pH 7.1, 37 °C. Lane* are the ligands in the absence of metal ion. Lane C is the DNA control in the absence of additives. The gel has been loaded immediately after preparation of the different solution without incubation time.

the control compound tach and the ligands **1**–**5** in the presence/absence of 1 eq. of Zn(II).

By increasing the concentration of the Zn(II) complexes, the signal corresponding to DNA gradually disappears from the gel. This behavior is likely a consequence of the binding of the conjugates to the DNA which induces aggregation/precipitation of the plasmid, thus preventing its entrance in the gel. Interestingly, the same effect is observed also in the absence of metal ion at least at the highest tested conjugate concentration Additionally, Zn(II)-tach complex, which binds to DNA only through electrostatic interactions, requires a higher concentration to exert the same effect. Taken together, this experimental evidence suggests the involvement of the minor groove binder in the process. Among the tested Zn(II) complexes the ranking order **2** ~ **3** > **4** ~ **5** > **1** describes the efficiency of the compounds in inducing the DNA fading effect, which should, at least qualitatively, correlate to their ability to bind to DNA leading to its precipitation. This corresponds to a higher efficiency for conjugates with a 4 and 6 methylene linker and, at parity of linker length, for the $(indole)_2$ vs benzofurane-indole moiety.

The loss of bands in the gel was induced also by conjugates **6**–**8** (data not shown). However, in this case higher concentrations (20–50 μM) were required to fully prevent DNA visualization. This supports a contribution of the hydrophobic linker to the process which becomes less relevant when the more polar oxyethylene linker is included. Noteworthy, the presence of two $(indole)_2$ subunits in compound **8** reduced the concentration at which DNA is not any more detectable.

Fortunately, the observed fading effect of DNA was due to a reversible binding of our conjugates on the nucleic acid. Indeed, results shown in Fig. 4 clearly support the observation that the addition to the samples of an excess of EDTA and SDS before loading hampers the complexation of the conjugates, and restores the normal mobility of the plasmid DNA.

To confirm a correlation between the observed effect on the electrophoretic mobility of the DNA with the binding of our ligands to the macromolecule, we performed UV-VIS titrations. In particular, we monitored the absorption properties of our conjugates in the presence of increasing concentrations of calf thymus DNA (ctDNA). An example is reported in Fig. 5.

Addition of the nucleic acid to the tested binders reduced the intensity of the absorption band of the ligands either in the presence or in the absence of coordinated metal ions (Zn(II) or Cu(II)). The affinity of the binder for the nucleic acid was remarkable although the binding event is complex as suggested by the different shape of the binding isotherms (Fig. 5B). This may be the result of several factors such as, for example, different binding stoichiometry or different aggregation state of the ligands which were not further investigated. Therefore, for a meaningful comparison we report in Table 1 the concentration required to induce 50% of the maximal observed absorbance variation at a constant wavelength, which we can be referred as an effective concentration at 50% of the binding event (EC_{50}).

Data in Table 1 show that metal ion coordination actually improves the recognition of the double helix lowering the EC_{50} by a factor of about 2. On the other hand, compounds **4** and **5** exhibited comparable EC_{50}. This suggests that the substitution of the $(indole)_2$ amide with a benzofuran-indole amide doesn't impair the formation of the complex. Conversely, the presence of the oxyethylene linker reduces the affinity of the ligand (compare compounds **4** and **7**). Interestingly, moving from one $(indole)_2$ binding moiety (compound **7**) to two (compound **8**) a two fold reduction of the EC_{50} was determined, thus ruling out cooperative binding of the two minor groove moieties to DNA.

All these data correlate with the different behavior of our conjugates on DNA migration, thus supporting the observed fading of plasmid DNA in the gel being related to the interaction of our ligands with the nucleic acid.

To assess the DNA binding mode of the conjugates, we acquired the CD spectra of ctDNA in the presence of **4**, Zn(II)-**4** or Cu(II)-**4** (Fig. 6). In agreement with the above described efficient recognition of the macromolecule, addition of **4** leads to a significant change in the dichroic features of the nucleic acid. In particular, a relevant positive induced CD contribution appears in the ligand absorption region. This is indicative of its binding in the minor groove. It is

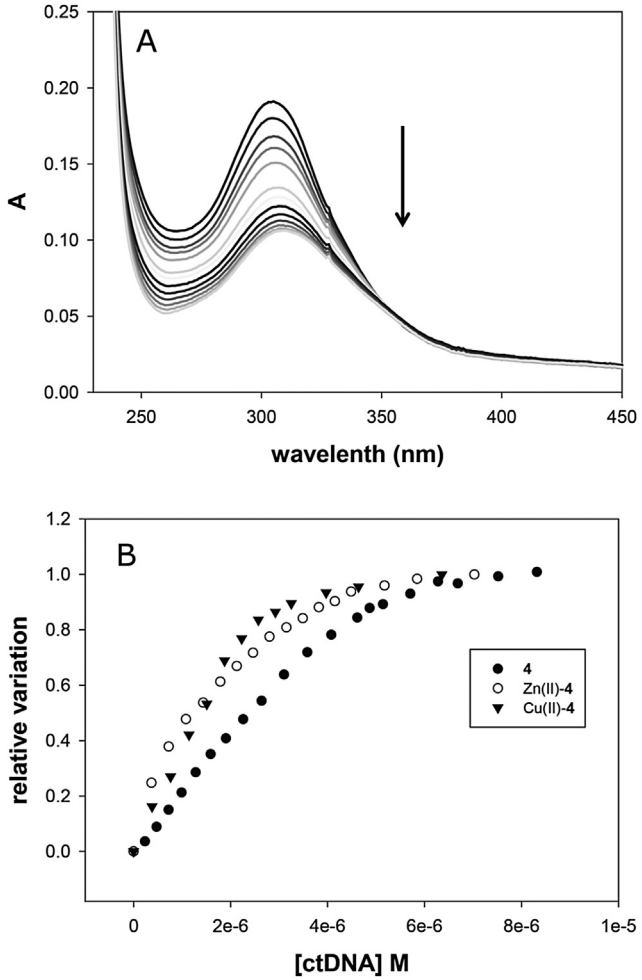

Fig. 5. Variation of the absorption spectrum of **4** (37 μM) induced by addition of ctDNA in 20 mM HEPES, pH 7.1 (PANEL A). Arrow indicates the effect of increasing ctDNA concentrations. In PANEL B the relative variation of the absorbance of **4** alone, Zn(II)-**4** or Cu(II)-**4** recorded at 305 nm is reported as a function of nucleic acid concentration.

worth noting that complexation of **4** with Zn(II) or Cu(II) did not significantly rearrange the ligand within the groove. Indeed, the positive signal is preserved in each case.

Once we demonstrated that the Zn(II) complexes of the conjugates bind DNA, their ability to cleave DNA was investigated. We checked this activity by following the formation of a cleaved site on pBR322 upon a 24 h incubation at 37 °C in HEPES buffer pH 7.1 and by resolving the reaction products by agarose gel electrophoresis in the presence of SDS to dissociate the metal complexes from the nucleic acid. In these experimental conditions, DNA cleavage

Table 1
EC_{50} (μM) values determined for the tested derivatives by UV-VIS titrations with ctDNA in 20 mM HEPES, pH 7.1.

	EC_{50} (μM)
4	2.60 ± 0.27
Zn(II)-**4**	1.45 ± 0.10
Cu(II)-**4**	1.49 ± 0.13
5	2.70 ± 0.09
7	3.13 ± 0.05
8	1.44 ± 0.07

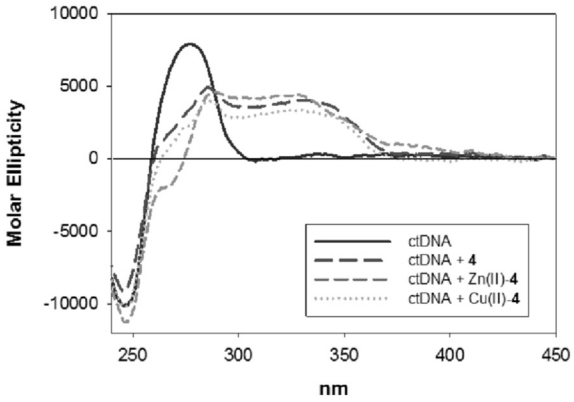

Fig. 6. CD spectra of ctDNA alone and in the presence of **4**, Zn(II)-**4** or Cu(II)-**4** recorded in 20 mM HEPES, pH 7.1.

should result in a decrease of the intensity of the band corresponding to the supercoiled DNA and in the appearance of the spots of nicked and eventually linear DNA. Disappointingly, the Zn(II) complexes of the tested conjugates did not show any ability to cleave DNA up to a concentration of 200 μM. This is shown in Fig. 7 (top) for complexes **6**–**8** but comparable results were obtained with complexes **1**–**5**. The activity of the Zn(II) complexes of the conjugates is even lower than that of the Zn(II)-tach complex which is known to cleave plasmid DNA at concentrations above 100 μM under the same experimental conditions.[8] Therefore, the conjugation of the Zn(II)-tach to the minor groove binders led not to an increase, but to an inhibition of the hydrolytic activity of the metal complex. To confirm this effect, the DNA cleavage produced by the complex of ligands **6**–**8** with the more active Cu(II) metal ion was investigated. The results shown in Fig. 7 (bottom) showed cleavage activity only at high concentration while, in the same experimental conditions, the Cu(II)-tach complex is reported to fully nick plasmid at concentration below 20 μM.[29] Therefore, also in this case, the conjugation of the metal complex to the minor groove binder is detrimental for its DNA cleaving activity.

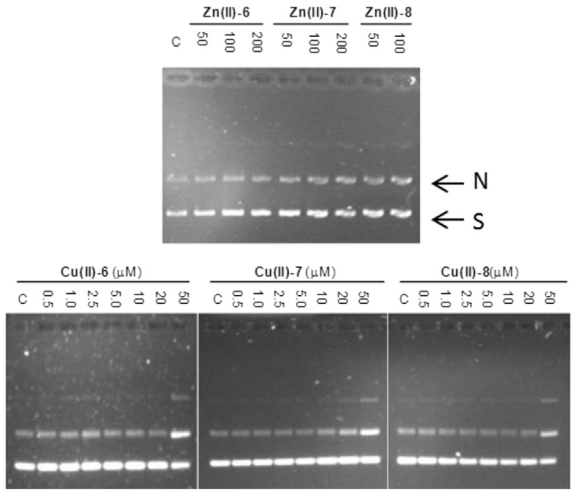

Fig. 7. Top: Agarose gel electrophoresis of pBR 322 DNA (12 μM) after 24 h incubation with the indicated concentration of the Zn(II) complexes of ligands **6**–**8** in 20 mM HEPES, pH 7.1, 37 °C. Bottom: Agarose gel electrophoresis of pBR 322 DNA (12 μM) after 3 h incubation with the indicated concentration of the Cu(II) complexes of ligands **6**–**8** in 20 mM HEPES, pH 7.0, 37 °C. Lane C is DNA incubated in the absence of complexes. Before loading, samples were added of EDTA and SDS. S and N refer to the supercoiled and nicked plasmid DNA, respectively.

2.3. Molecular modeling of DNA conjugates complexes

The data illustrated above indicate that the Zn(II) complexes of the tach conjugates are able to bind but not cleave plasmid DNA. To get insight into such behavior, molecular mechanics calculations were performed on the complexes between B-DNA and Zn(II)-**3** and Zn(II)-**8**. In the case of Zn(II)-**3** (Fig. 8) the optimized structure of the complex shows the $(indole)_2$ subunit deeply inserted in the DNA minor groove. The C6-linker which is attached to one extremity of the $(indole)_2$ follows the minor groove curvature, and it is also deeply inserted in the groove establishing stabilizing hydrophobic interactions between the alkyl chain and the DNA. In this conformation the appended Zn(II)-tach complex is not able to get close to the phosphate backbone, and this unfavorable geometry hampers the interaction between the metal ion and the phosphate group leading to inhibition of the cleavage process. Therefore the design of the conjugates in which the binder, the linker and the metal complex are arranged in a linear fashion seems to lead to unproductive binding modes, because the conjugate is buried in the minor groove and the metal complex is not able to reach the phosphate backbone.

The less predictable result obtained in the cleavage of DNA was the inactivity of the hairpin derivative Zn(II)-**8**. This dimeric compound was indeed prepared with the hope, based on modeling studies, that the tweezer like binding mode of the two $(indole)_2$ subunits should force the Zn(II)-tach complex close to the phosphate groups of DNA. This is illustrated in the modeled structure of Fig. 9 (left), in which the favorable orientation of the metal complex is evident. However, the same calculation suggested the possibility of a less favorable binding mode in which the metal complex is turned away from the DNA pointing toward the exterior of the minor groove well distant from the phosphate backbone as shown in Fig. 9 (right). Clearly, the experimental results indicate that this second unproductive binding mode prevails.

3. Conclusions

In this paper we have presented the synthesis of a new class of conjugates between a Zn(II)-tach complex and $(indole)_2$ or benzofuran-indole amide minor groove binders connected through alkyl or ethoxyethyl linkers. The conjugates strongly bind DNA and the binding strength is influenced by the nature and length of the linkers. This suggests that not only the tach unit, which both in the free and in the Zn(II) complex form can provide additional electrostatic interaction with the phosphate backbone, but also the linker can have an effect on the DNA affinity of the conjugates. Surprisingly, the complexation to DNA instead of promoting the Zn(II) catalyzed hydrolytic cleavage of the DNA results in its inhibition with the Zn(II)-tach conjugates being less effective than the isolated Zn(II)-tach complex, regardless of the length and nature of the linker. This inhibition effect has been confirmed also using Cu(II) as metal ion. Modeling studies suggest that in the most stable complex conformation the minor groove binder and the linker lie in the minor groove hampering the interaction between the metal complex and the phosphate backbone of DNA. Interestingly, the hydrophobic interaction of the linker with the minor groove is stronger than the electrostatic/coordination interaction of Zn(II) with the phosphate groups. Therefore, the linear arrangement of minor groove binder-linker-metal complex appears to be unproductive from a hydrolytic point of view. This may also explain the relatively low reactivity of the system reported by Qiao and Zhao which, although with different minor groove binders and metal complexes, presents the same linear arrangement of the catalyst components[25,26] and also suggests a strategy for increasing the DNA affinity of minor groove binders. On this basis, we believe that active hydrolytic catalysts may be obtained by changing the topology of the conjugates and in particular by attaching the linker to a position on the minor groove binder subunit such as to force the linker itself to exit the minor groove allowing the positioning of the metal complex close to the phosphate group. Work is progress to prepare new conjugates in order to verify this hypothesis.

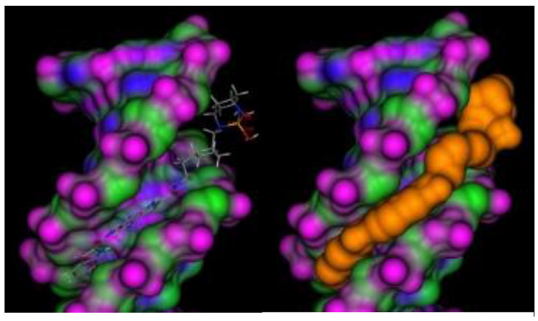

Fig. 8. Modeled structure of the complexes between Zn(II)-**3** and DNA. DNA structure is represented using its Connolly's surface while the interacting molecule as stick (left) and Connolly's surface (right).

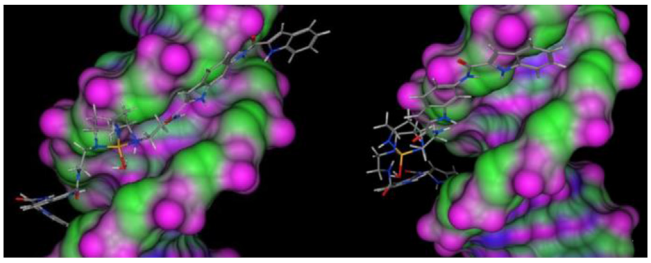

Fig. 9. Modeled structures of two different complexes between Zn(II)-**8** and DNA. DNA structure is represented using its Connolly's surface.

4. Experimental section

All commercially available reagents were purchased from *Aldrich*, *Fluka* and *Strem Chemicals* and used without purification unless otherwise mentioned. Solvents were purchased from *Aldrich*, *VWR*, *Fluka* and *Riedel*, and deuterated solvents from *Cambridge Isotope Laboratories* and *Aldrich*. Reactions were routinely monitored by thin-layer chromatography (TLC) on silica gel (precoated F_{254} *Merck* plates). Chromatography was performed on *Merck* silica gel 60F-254 (230÷400 Mesh) and the solvents employed were of analytical grade. NMR spectra were recorded on a Jeol 400 spectrometer (operating at 400 MHz for proton and at 100 MHz for carbon) or on Jeol X-270 (operating at 270 MHz for proton and at 67.8 MHz for carbon). Chemical shifts (δ) are reported in ppm using the solvent residual signal as an internal reference. Coupling constants (J) are quoted in Hz. The letter in brackets in the ^{13}C NMR spectra description is the multiplicity of the carbon atom as determined from DEPT experiments (s = singlet, d = doublet, t = triplet, q = quartet). Electrospray mass spectra were recorded on a *Perkin Elmer* APII spectrometer. HRMS spectra were recorded on a Perceptive Biosystems ABI Mariner ESI-TOF instrument. Infrared spectra (IR) were recorded with a Nicolet Nexus 870 instrument operating in the ATR mode on a diamond crystal. *All-cis*-3,5-*N*,*N*-di-*tert*-butyloxycarbonyl-1-*N*-(4-aminobutyl)-1,3,5-triaminocyclohexane[8] (**10**), *All-cis*-3,5-*N*,*N*-di-*tert*-butyloxycarbonyl-1-*N*-(6-aminohexyl)-1,3,5-triaminocyclohexane[8] (**11**), *All-cis*-3,5-*N*,*N*-di-*tert*-butyloxycarbonyl-1-*N*-(8-aminooctyl)-1,3,5-

triaminocyclohexane (**12**),[8] *N*-Benzyloxycarbonyl-2-bromo-ethylamine (**15**),[30] *All-cis*-3,5-*N*,*N*-di-*tert*-Butyloxycarbonyl-1,3,5-triaminocyclohexane (**21**, tach-DIBOC[8]), *All-cis*-5-*N*-*tert*-Butyloxycarbonyl-1,3,5-triaminocyclohexane (**28**, tach-MONOBOC[8]), 5-[((1H-Indol-2'-yl)carbonyl)amino]-lH-indole-2-carboxylic acid[28] (**31**), 5-[((Benzofuro-2'-yl)carbonyl)amino]-1H-indole-2-carboxylic acid[28] (**32**), were synthesized as reported.

*4.1. N-Benzyloxycarbonyl-ω-bromo-1-alkyloxyamine **19**–**20***

The desired aminoalcohol (17 mmol, 2-(2-aminoethoxy)ethanol or 2-[2-(2-aminoethoxy)ethoxy]ethanol) was dissolved in CH_3OH (10 mL) and TEA (5.45 mL, 39.2 mmol) was added. To this solution, stirred at room temperature, was added dropwise a solution of benzyloxycarbonyl chloride (ZCl, 3.2 g, 18.77 mmol) in CH_3OH (5 mL). After the addition was complete the reaction mixture was stirred at room temperature for 20 h, protected from moisture with a $CaCl_2$ drying tube. The solvent was then evaporated and the crude was dissolved in CH_2Cl_2 (150 mL) and washed first with a 5% aqueous solution of $KHSO_4$ (2 × 50 mL) and then with water (2 × 50 mL). The evaporation of the dried solvent (Na_2SO_4) afforded the product as a clear oil pure enough to be used in the following steps.

4.1.1. 2-(N-Benzyloxycarbonyl-2-aminoethoxy)ethanol[31]

Yield 85%; $R_f = 0.35$ (CH_2Cl_2/CH_3OH 9.5:0.5); ^{1}H NMR ($CDCl_3$) δ: 2.58 (br, 1H); 3.39 (q, 2H, $J = 5.6$ Hz); 3.52–3.59 (m, 4H); 3.69–3.76 (m, 2H); 5.09 (s, 2H); 5.42 (br, 1H); 7.31–7.35 (m, 5H); ^{13}C NMR ($CDCl_3$) δ: 40.8 (t); 61.6 (t); 66.7 (t); 70.1 (d); 72.2 (d); 128.1 (d); 128.5 (d); 136.4 (s); 156.6 (s); ESI-MS (*m*/*z*): 240.0 [M + H^+]; 262.0 [M + Na^+]; 278.0 [M + K^+]; 257.0 [M + NH_4^+].

4.1.2. 2-[2-(N-Benzyloxycarbonyl-2-aminoethoxy)ethoxy]ethanol[32]

Yield 90%. $R_f = 0.30$ (CH_2Cl_2/CH_3OH 9.5:0.5); ^{1}H NMR, ($CDCl_3$) δ: 2.38 (br, 1H); 3.41 (q, 2H, $J = 6.2$ Hz); 3.54–3.61 (m, 8H); 3.75–3.83 (m, 2H); 5.10 (s, 2H); 5.39 (br, 1H); 7.32–7.38 (m, 5H); ^{13}C NMR, ($CDCl_3$) δ: 40.8 (t); 61.5 (t), 66.6 (t); 69.8 (t); 71.4 (t); 128.1 (d); 128.4 (d); 136.5 (s); 156.4 (s); ESI-MS (*m*/*z*): 284.3 [M + H^+]; 306.0 [M + Na^+]; 322.3 [M + K^+]; 301.2 [M + NH_4^+].

The above protected aminoalcohol (2 mmol) was dissolved in CH_2Cl_2 (15 mL) and CBr_4 (0.990 g, 2.98 mmol) and Ph_3P (0.783 g, 2.98 mmol) were added to the stirred solution at 0 °C. The solution was warmed at room temperature and the reaction was followed by TLC (Petroleum ether/EtOAc 7/3). After 90 min at r.t. water was added in the reaction flask. The solution was diluted with CH_2Cl_2 (110 mL) and the organic phase was washed twice with water and brine, dried over Na_2SO_4 and the solvent evaporated to dryness under vacuum. The crude material was purified by flash chromatography (SiO_2, petroleum ether/AcOEt 90/10, gradient 2%) to give the bromide as a transparent oil.

*4.1.3. 2-(N-Benzyloxycarbonyl-2-aminoethoxy)-1-bromo-ethane (**19**)*

Yield 77%; R_f = 0.4 (petroleum ether/AcOEt 6:4); ^{1}H NMR, ($CDCl_3$) δ: 3.41 (q, 2H, $J = 5.2$ Hz); 3.45 (t, 2H, $J = 6.0$ Hz); 3.57 (t, 2H, $J = 5.2$ Hz); 3.76 (t, 2H, $J = 6.0$ Hz); 5.11 (s, 2H); 7.32–7.36 (m, 5H); ^{13}C NMR, ($CDCl_3$) δ: 30.3 (t); 40.7 (t); 66.5 (t); 69.7 (t); 70.6 (t); 127.9 (d); 128.2 (d); 136.4 (s); 156.3 (s). ESI-MS (*m*/*z*): 304.0 [M + H^+]; 324.1 [M + Na^+]; 340.0 [M + K^+]; 318.9 [M + NH_4^+].

*4.1.4. 2-[2-(N-Benzyloxycarbonyl-2-aminoethoxy)ethoxy]-1-bromo-ethane (**20**)*

Yield 64%; R_f = 0.35 (petroleum ether/AcOEt 6:4); ^{1}H NMR, ($CDCl_3$) δ: 3.39 (q, 2H, $J = 5.0$ Hz); 3.45 (t, 2H, $J = 6.1$ Hz); 3.57 (t, 2H, $J = 5.0$ Hz); 3.60–3,67 (m, 4H); 3.79 (t, 2H, $J = 6.1$ Hz); 5.14 (s, 2H); 7.28–7.39 (m, 5H). ^{13}C NMR, ($CDCl_3$), δ: 30.2 (t); 40.8 (t); 66.6 (t); 70.1 (t); 70.3 (t); 71.1 (t); 128.0 (dd); 128.4 (d); 136.5 (s); 156.3 (s). ESI-MS (*m*/*z*): 348.2 [M + H^+]; 369.9 [M + Na^+]; 386.1 [M + K^+]; 364.9 [M + NH_4^+].

*4.2. General synthesis of All-cis-3,5-N,N-di-tert-butyloxycarbonyl-1-N-[ω- N-(benzyloxycarboyl)aminoalkyl/alkyloxy]-1,3,5-triaminocyclohexane derivatives (**22**–**27**)*

To a solution of tach-DIBOC (**21**, 250 mg, 0.76 mmol) in dry CH_3CN (18 mL) were added 1.3 eq. of the appropriate amino bromo derivative (**15**–**20**) and *N*-diisopropylethylamine (DIPEA, 132 μl, 0.76 mmoli). The obtained mixture was refluxed for 8 days and the reaction monitored by TLC ($CHCl_3$/MeOH/NH_3 9.5:0.5:0.1). Then the solvent was removed under reduced pressure, the residue dissolved in $CHCl_3$ (35 mL) and washed three times with saturated $NaHCO_3$ (10 mL). The organic phase was dried over Na_2SO_4, concentrated and the crude residue was purified by flash chromatography (SiO_2, $CHCl_3$/MeOH/NH_3 98:1:1) to afford the final compounds in a good yield.

*4.2.1. All-cis-3,5-N,N-di-tert-butyloxycarbonyl-1-N-[**2**- N-(benzyloxycarboyl)aminoethyl]-1,3,5-triamino-cyclohexane (**22**)*

Yield 42%; white solid, mp 188 °C; $R_f = 0.6$ ($CHCl_3$/MeOH/NH_3 9.5:0.5:0.1); ^{1}H NMR ($CDCl_3$) δ: 0.86 (dd, 3H, $J_1 = J_2 = 11.8$ Hz); 1.35 (s, 18H); 2.13–2.24 (m, 3H); 2.52–2.60 (m, 1H); 2.74 (q, 2H, $J = 5.5$ Hz); 3.25 (q, 2H, $J = 5.5$ Hz); 3.52 (br, 2H); 4.42 (br, 2H); 5.09 (s, 2H); 5.18 (brs, 1H); 7.22–7.39 (m, 5H); ^{13}C NMR ($CDCl_3$) δ: 28.4 (q); 39.9 (t); 41.3 (t, 3C); 46.3 (t); 46.7 (d, 2C); 53.4 (d); 66.7 (t); 79.4 (s); 128.1 (d, 2C); 128.2 (d); 128.5 (d, 2C); 136.5 (s); 154.9 (s); 156.5 (s); ESI-MS (*m*/*z*): 507.2 [M + H^+].

*4.2.2. All-cis-3,5-N,N-di-tert-butyloxycarbonyl-1-N-[2-(N-Benzyloxycarbonyl-2-aminoethoxy)ethyl]-1,3,5-triaminocyclohexane (**26**)*

Yield 42%; white solid; $R_f = 0.22$ ($CHCl_3/CH_3OH/NH_3$ 9:1:0.1); ^{1}H NMR ($CDCl_3$) δ: 0.84 (dd, 3H, $J_1 = J_2 = 10.9$ Hz); 1.45 (s, 18H); 2.15 (bs, 3H); 2.56 (t, 1H, $J = 11.2$ Hz); 2.75 (t, 2H, $J = 4.8$ Hz); 3.35 (q, 2H, $J = 4.8$ Hz); 3.52 (br, 6H); 4.40 (bs, 2H); 5.09 (s, 2H); 5.54 (bs, 1H); 7.24–7.40 (m, 5H); ^{13}C NMR, ($CDCl_3$) δ: 28.3 (q); 39.5 (2t, 2C); 41.0 (2t, 2C); 47.2 (2d, 2C); 47.3 (t); 53.5 (d); 66.5 (t); 69.6 (t); 70.2 (t); 79.3 (s); 128.0 (d, 2C); 128.1 (d, 1C); 128.4 (d, 2C); 136.5 (s, 1C); 154.9 (s, 2C); 156.4 (s); ESI-MS (*m*/*z*): 552.2 [M + H^+]; 573.8 [M + Na^+]; 589.4 [M + NH_4^+].

*4.2.3. All-cis-3,5-N,N-di-tert-butyloxycarbonyl-1-N-{2-[2-(N-Benzyloxycarbonyl-2-aminoethoxy)ethoxy]ethyl}-1,3,5-triaminocyclohexane (**27**)*

Yield 49%; white solid, $R_f = 0.35$ ($CHCl_3/CH_3OH/NH_3$ 9:1:0.1); ^{1}H NMR, ($CDCl_3$) δ: 0.84 (dd, 3H, $J_1 = J_2 = 11.5$ Hz); 1.50 (s, 18H); 2.11–2.19 (m, 3H); 2.57 (t, 1H, $J = 11.2$ Hz); 2.76 (t, 2H, $J = 4.6$ Hz); 3.38 (q, 2H, $J = 5.0$ Hz); 3.51–3.62 (m, 10H); 4.40 (bs, 2H); 5.08 (s, 2H); 5.63 (bs, 1H); 7.28–7.37 (m, 5H); ^{13}C NMR, ($CDCl_3$) δ: 27.8 (q); 39.1 (2t, 2C); 40.3 (2t, 2C); 46.3 (2d, 2C); 46.4 (t); 52.8 (d); 66.1 (t); 69.5 (t, 2C); 70.0 (t, 2C); 78.6 (s); 128.1 (dd, 5C); 136.2 (s, 1C); 154.9 (s, 2C); 156.0 (s); ESI-MS (*m*/*z*): 595.4 [M + H^+]; 617.3 [M + Na^+].

*4.3. Synthesis of All-cis-5-N-tert-butyloxycarbonyl-1,3-N,N-di-[2-(N-Benzyloxycarbonyl-2-aminoethoxy)ethyl]-1,3,5-triamino-cyclohexane (**29**)*

To a solution of tach-MONOBOC (**28**, 121 mg, 0.53 mmol) in dry CH_3CN (10 mL) were added 2 eq. of Br–$(CH_2)_2$–O–$(CH_2)_2$–NH-Z (**19**) and DIPEA (185 μl, 1.06 mmol). The obtained mixture was refluxed for 4 days and the reaction monitored by TLC ($CHCl_3$/MeOH/NH_3 9:1:0.2). Then the solvent was removed under reduced

pressure, and the residue dissolved in $CHCl_3$ (30 mL) and washed three times with 5% $NaHCO_3$ (10 mL) and one time with brine (10 mL). The organic phase was dried, concentrated and the crude residue was purified by flash chromatography (SiO_2, $CHCl_3$/MeOH/NH_3 100:0.5:1) to afford 107 mg of the final compound (**29**) as a yellow oil with a 30% yield. R_f: 0.8 ($CHCl_3$/MeOH/NH_3 9.5:0.5:0.1); ^{1}H NMR, ($CDCl_3$), δ: 0.84 (dd, 3H, $J_1 = J_2 = 11.2$ Hz); 1.41 (s, 9H), 2.08 (d, 1H, $J = 11.4$ Hz); 2.16 (d, 2H, $J = 11.4$ Hz); 2.54 (t, 2H, $J = 11.2$ Hz); 2.72–2.80 (m, 4H); 3.33–3.56 (m, 13H); 4.35 (bs, 1H); 5.10 (s, 4H); 5.35 (bs, 2H); 7.25–7.38 (m, 10H); ^{13}C NMR, ($CDCl_3$), δ: 28.4 (q); 39.65 (t, 2C); 39.85 (t); 40.86 (t); 46.43 (t); 46.74 (d); 53.73 (d, 2C); 66.61 (t, 2C); 69.72 (t, 2C); 70.26 (t, 2C); 79.3 (s); 128.27 (dd); 136.58 (s, 1C); 155.07 (s); 156.4 (s); ESI-MS (m/z): 672.6 [M + H^+]; 694.5 [M + Na^+].

4.4. General procedure for Z-deprotection (**9**–**14**, **30**)

To a methanolic (15 mL) solution containing 0.2 mmol of the appropriate Z-protected ligands (**22**–**27, 29**) was added a catalytic amount (20 mg) of 5% PdC. The resulting mixture was stirred under hydrogen atmosphere for 2 h. The reaction was monitored by TLC ($CHCl_3$/MeOH/NH_3 9:1:0.1). Then the catalyst was filtered off and the solvent removed under reduced pressure affording the desired final compounds (**9**–**14, 30**) in a good yield.

4.4.1. All-cis-3,5-N,N-di-tert-butyloxycarbonyl-1-N-(2-aminoethyl)-1,3,5-triamino-cyclohexane (**9**)

Yield 76%; white solid; Rf = 0.1 ($CHCl_3$/MeOH/NH_3 9:1:0.1); ^{1}H NMR (DMSO) δ: 1.17 (dd, 3H, $J_1 = J_2 = 11.9$ Hz); 1.36 (s, 18H); 1.92 (dd, 3H, $J_1 = J_2 = 11.9$ Hz); 3.07–3.16 (m, 3H); 3.27–3.38 (m, 4H); 7.04 (bs, 2H); ESI-MS (m/z): 373.3 [M + H^+].

4.4.2. All-cis-3,5-N,N-di-tert-butyloxycarbonyl-1-N-[2-(2-aminoethoxy)ethyl]-1,3,5-triaminocyclohexane (**13**)

Yield 84%; white solid; ^{1}H NMR ($CDCl_3$) δ: 0.91 (dd, 3H, $J_1 = J_2 = 11.5$ Hz); 1.37 (s, 18H); 2.14–2.26 (m, 3H); 2.58–2.66 (m, 1H); 2.74–2.83 (m, 2H); 2.86 (t, 2H, $J = 5.3$ Hz); 3.47 (t, 2H, $J = 5.3$ Hz); 3.51–3.62 (m, 4H); 4.42 (bs, 2H).

4.4.3. All-cis-3,5-N,N-di-tert-butyloxycarbonyl-1-N-{2-[2-(2-aminoethoxy)ethoxy]ethyl}-1,3,5-triaminocyclohexane (**14**)

Yield 76%; white solid; ^{1}H NMR ($CDCl_3$) δ: 0.88 (dd, 3H, $J_1 = J_2$ 11.7 Hz); 1.36 (s, 18H); 2.13–2.25 (m, 3H); 2.59 (t, 1H, $J = 11.2$ Hz); 2.78 (t, 2H, $J = 5.15$ Hz); 3.48 (t, 2H, $J = 5.13$ Hz); 3.51–3.65 (m, 10H); 4.42 (bs, 2H).

4.4.4. All-cis-5-N-tert-butyloxycarbonyl-1,3-N,N-di-[2-(2-aminoethoxy)ethyl]-1,3,5-triamino-cyclohexane (**30**)

Yield 71%, white solid; ^{1}H NMR ($CDCl_3$) δ: 0.87 (dd, 3H, $J_1 = J_2 = 11.5$ Hz); 1.40 (s, 9H); 2.10 (dd, 3H, $J_1 = J_2 = 11.4$); 2.53 (t, 1H, J = 11.5); 2.72–2.83 (m, 6H); 3.40–3.54 (m, 12H); 4.71 (bs, 1H).

4.5. General synthesis of conjugates between minor groove binders and tach derivatives (**33**–**39**)

A DMF (3 mL) solution of acid derivatives (**31**, **32**, 0.188 mmol, 1.2 eq), EDCI (60 mg, 2 eq) TACH derivative (**9**–**14**, 0.156 mmol) and Et_3N (21 μL) was stirred at room temperature for 2 days and monitored by TLC (CH_2Cl_2/MeOH/NH_3 8.5:1.5:0.1). Then the solvent was removed in vacuo, and the residue treated with water (40 mL). The aqueous solution was extracted with EtOAc (3 × 25 mL), and the combined organic phases dried and concentrated under reduced pressure. The crude residue was purified by flash chromatography (CH_2Cl_2/MeOH/NH_3 100:0.5:1) to afford the final compounds **33**–**39** in moderate yield.

4.5.1. (Indole)$_2$-C$_2$-tach-DIBOC (**33**)

Yield 30.6%; pale yellow solid; mp 276 °C; Rf = 0.6 (CH_2Cl_2/MeOH/NH_3 8.5:1.5:0.1); ^{1}H NMR (DMSO) δ: 0.84 (dd, 2H, $J_1 = J_2 = 11.6$ Hz); 0.99 (dd, 1H, $J_1 = J_2 = 11.6$ Hz); 1.37 (s, 18H); 1.81 (d, 1H, $J = 11.4$ Hz); 1.92 (d, 2H, $J = 11.4$ Hz); 2.50–2.61 (m, 1H); 2.65–2.76 (m, 2H); 3.19–3.39 (m, 4H); 6.86 (d, 1H, $J = 8.0$ Hz); 7.06 (t, 1H, $J = 8.0$ Hz); 7.09 (s, 1H); 7.21 (t, 1H, $J = 8.0$ Hz); 7.37–7.53 (m, 3H); 7.67 (d, 1H, $J = 8.0$ Hz); 8.10 (s, 1H); 8.43 (bs, 1H); 10.13 (s, 1H); 11.58 (bs, 1H); 11.70 (bs, 1H); ^{13}C NMR (DMSO) δ: 28.4 (q); 46.0 (t); 46.4 (d, 2C); 53.3 (d); 77.5 (s, 2C); 102.5 (d), 103.4 (d); 112.3 (d); 112.4 (d); 112.8 (d); 118.5 (d); 119.9 (d); 121.7(d); 123.6 (d); 126.9 (s); 127.2 (s); 131.5 (s); 132.0 (s); 133.3 (s); 133.6 (s); 136.7 (s); 154.8 (s, 2C); 159.5 (s); 161.2 (s); ESI-MS (m/z): 674.4 [M + H^+].

4.5.2. (Indole)$_2$-C$_4$-tach-DIBOC (**34**)

Yield 20.6%; pink solid; mp 225 °C; R_f = 0.6 (CH_2Cl_2/MeOH/NH_3 8.5:0.5:0.1); ^{1}H NMR (CD_3OD) δ: 0.99 (dd, 2H, $J_1 = J_2 = 11.6$ Hz); 1.06 (dd, 1H, $J_1 = J_2 = 11.6$ Hz); 1.39 (s, 18H); 1.56–1.72 (m, 4H); 2.01 (d, 1H, $J = 11.4$ Hz); 2.11 (d, 2H, $J = 11.4$ Hz); 2.64–2.72 (m, 3H); 3.32–3.44 (m, 4H); 7.01–7.12 (m, 2H); 7.20 (t, 1H, $J = 8.0$ Hz); 7.26 (s, 1H); 7.36–7.48 (m, 3H); 7.61 (d, 1H, $J = 8.1$ Hz); 7.98 (s, 1H); ^{13}C NMR (CD_3OD) δ: 27.5 (t); 28.5 (t); 28.9 (q); 38.9 (t); 40.3 (t, 3C); 47.3 (t); 48.0 (d, 2C); 55.0 (d); 80.2 (s, 2C); 104.3 (d); 105.0 (d); 113.2 (d, 2C); 115.5 (d); 120.8 (d); 121.3 (d); 123.0 (d); 125.3 (d); 129.1 (s, 2C); 132.4 (s, 2C); 133.4 (s); 135.9 (s); 138.6 (s); 157.7 (s, 2C); 162.6 (s); 164.1 (s); MS-ESI (m/z): 702.4 [M + H^+].

4.5.3. (Indole)$_2$-C$_6$-tach-DIBOC (**35**)

Yield 18%; white solid; mp 221 °C; R_f = 0.6 (CH_2Cl_2/MeOH/NH_3 8.5:1.5:0.1); ^{1}H NMR (CD_3OD) δ: 0.92 (dd, 2H, $J_1 = J_2 = 11.7$ Hz); 1.03 (dd, 1H, $J_1 = J_2 = 11.7$ Hz); 1.20–1.51 (m, 24H); 1.56–1.65 (m, 2H); 1.92–2.08 (m, 3H); 2.49–2.61 (m, 3H); 3.30–3.42 (m, 4H); 6.95–7.14 (m, 2H); 7.20 (t, 1H, $J = 7.9$ Hz); 7.27 (s, 1H); 7.34–7.51 (m, 3H); 7.60 (d, 1H, $J = 7.9$ Hz); 7.98 (s, 1H); ^{13}C NMR (CD_3OD) δ: 22.0 (t); 27.4 (q); 28.9 (t); 29.1 (t, 2C); 37.7 (t); 37.8 (t); 39.0 (t, 2C); 46.2 (t); 46.6 (d, 2C); 53.5 (d); 78.6 (s, 2C); 102.8 (d); 103.5 (d); 111.8 (d, 2C); 114.0 (d); 119.2 (d); 119.8 (d); 121.4 (d); 123.7 (d); 127.7 (s, 2C); 131.0 (s, 2C); 132.0 (s); 134.4 (s); 137.1 (s); 156.2 (s, 2C); 162.5 (s, 2C); ESI-MS (m/z): 629.4 [M^+-2BOC]; 730.5 [M + H^+].

4.5.4. (Indole)$_2$-C$_8$-tach-DIBOC (**36**)

Yield 22.2%; white solid; mp 208 °C, R_f = 0.6 (CH_2Cl_2/MeOH/NH_3 8.5:1.5:0.1); ^{1}H NMR (CD_3OD) δ: 0.89–1.04 (m, 3H); 1.34–1.59 (m, 28H); 1.64–1.71 (m, 2H); 2.02–2.23 (m, 3H); 2.67–2.79 (m, 3H); 3.39–3.51 (m, 4H); 7.08–7.16 (m, 2H); 7.25–7.37 (m, 2H); 7.51–7.55 (m, 2H); 7.67–7.73 (m, 2H); 8.10 (s, 1H); ^{13}C NMR (CD_3OD) δ: 27.5 (t, 2C); 28.8 (q); 29.3 (t, 2C); 29.4 (t); 30.6 (t); 39.0 (t); 40.0 (t, 3C); 47.2 (t); 47.7 (d, 2C); 54.9 (d); 79.9 (s, 2C); 104.1 (d); 104.8 (d); 113.3 (d, 2C); 115.1 (d); 120.5 (d); 121.3 (d); 122.9 (d); 125.2 (d); 129.1 (s, 2C); 132.6 (s, 2C); 133.5 (s); 135.6 (s); 138.4 (s); 157.4 (s, 2C); 163.7 (s, 2C); ESI-MS (m/z): 758.4 [M + H^+].

4.5.5. Benzofuran-indole-C$_4$-tach-DIBOC (**37**)

Yield 20%; yellow solid; mp 183 °C; R_f = 0.7 (CH_2Cl_2/MeOH/NH_3 8.5:1.5:0.1); ^{1}H NMR (CD_3OD) δ: 1.01–1.14 (m, 3H); 1.38 (s, 18H); 1.61–1.70 (m, 4H); 1.98 (d, 1H, $J = 11.6$ Hz); 2.19 (d, 2H, $J = 11.6$ Hz); 2.81–2.92 (m, 3H); 3.33–3.43 (m, 4H); 7.03 (s, 1H); 7.29 (t, 1H, $J = 7.9$ Hz); 7.38–7.46 (m, 3H); 7.57 (s, 1H); 7.61 (d, 1H, $J = 8.0$ Hz); 7.71 (d, 1H, $J = 7.9$ Hz); 8.02 (s, 1H); ^{13}C NMR (CD_3OD) δ: 22.6 (t); 28.3 (t); 28.9 (q); 39.9 (t); 42.2 (t, 3C); 46.7 (t); 47.8 (d, 2C); 55.1 (d); 70.6 (s, 2C); 104.5 (d); 112.0 (d); 113.3 (d, 2C); 115.8 (d); 120.8 (d); 124.0 (d); 125.2 (d); 128.5 (d); 129.1 (s, 3C); 133.5 (s); 136.2 (s); 156.8 (s); 157.7 (s); 159.6 (s, 2C); 164.2 (s, 2C); ESI-MS (m/z): 703.2 [M + H^+].

*4.5.6. (Indole)$_2$-NH–CH$_2$–CH$_2$–O–CH$_2$–CH$_2$–NH-tach-DIBOC (**38**)*

Yield 17%; white solid; Rf: 0.39 (CH_2Cl_2/MeOH/NH_3 8.5:1.5:0.1); ^{1}H NMR (CD_3OD) δ: 0.96 (dd, 3H, $J_1 = J_2 = 11.5$ Hz); 1.40 (s, 18H); 1.96 (d, 1H, $J = 11.6$ Hz); 2.15 (d, 2H, $J = 11.6$ Hz); 2.49 (t, 1H, $J = 11.5$ Hz); 2.77 (t, 2H, $J = 5.15$ Hz); 3.24–3.40 (m, 2H); 3.51–3.65 (m, 6H); 7.02–7.11 (m, 2H); 7.22 (t, 1H, $J = 7.9$ Hz); 7.30 (s, 1H); 7.42–7.51 (m, 3H); 7.64 (d, 1H, $J = 8.0$ Hz); 8.01 (s, 1H); ^{13}C NMR (CD_3OD) δ: 32.7 (t) 40.2 (t); 43.6 (d, 2C); 45.9 (d, 2C); 46.9 (t, 2C); 50.0 (d); 66.9 (t); 71.6 (t); 79.2 (s) 104.8 (d); 105.1 (d); 113.1 (d); 113.4 (d); 115.7 (d); 121.1 (d); 121.3 (d); 122.9 (d); 125.3 (d); 129.1 (s, 2C); 132.4 (s, 2C); 133.4 (s); 136.0 (s); 138.6 (s); 155.4 (s); 160.5 (s); 162.1 (s); ESI-MS (m/z): 718.5 [M + H$^+$].

*4.5.7. (Indole)$_2$-NH–(CH$_2$–CH$_2$–O)$_2$–CH$_2$–CH$_2$–NH-tach-DIBOC (**39**)*

Yield 18%; pale yellow solid; R_f: 0.4 (CH_2Cl_2/MeOH/NH_3 8.5:1.5:0.1); ^{1}H NMR (CD_3OD/$CDCl_3$) δ: 0.93 (dd, 3H, $J_1 = J_2 = 11.5$ Hz); 1.31 (s, 18H); 1.93–1.99 (m, 3H); 2.40–2.50 (m, 1H); 2.69 (t, 2H, $J = 5.4$ Hz); 3.26–3.34 (m, 2H); 3.55–3.68 (m, 10H); 7.07 (t, 1H, $J = 8.0$ Hz); 7.10 (s, 1H); 7.23 (t, 1H, $J = 8.1$ Hz); 7.31 (s, 1H); 7.42–7.50 (m, 3H); 7.64 (d, 1H, $J = 8.0$ Hz); 7.84 (s, 1H); ^{13}C NMR (CD_3OD/$CDCl_3$) δ: 28.4 (t); 38.5 (t); 39.0 (t, 2C); 40.5 (d, 2C); 45.3 (t); 45.6 (d); 48.0 (t); 69.1 (t, 2C); 69.7 (t, 2C); 79.2 (s); 103.6 (d); 103.9 (d); 111.9 (d); 112.1 (d); 114.0 (d); 120.2 (d); 120.3 (d); 121.5 (d); 123.9 (d); 127.1 (s); 127.2 (s); 130.3 (s); 131.1 (s); 133.9 (s); 136.3 (s); 136.7 (s); 155.4 (s); 160.5 (s); 162.1 (s); ESI-MS (m/z): 762.4 [M + H$^+$].

*4.6. Synthesis of di-[(Indole)$_2$-NH–CH$_2$–CH$_2$–O–CH$_2$–CH$_2$–NH–]-tach-MONOBOC (**40**)*

A DMF (10 mL) solution of acid derivative **31** (0.489 mmol, 4 eq), EDCI (125 mg, 0.81 mmol, 6 eq), TACH derivative **30** (0.109 mmol, 1 eq) and Et_3N (61 μL) was stirred at room temperature for 2 days and monitored by TLC (CH_2Cl_2/MeOH/NH_3 8.5:1.5:0.1). Then the solvent was removed in vacuo and the residue treated with water (10 mL). The suspension was extracted with EtOAc (3 × 25 mL), and the combined organic phases dried and concentrate under reduced pressure. The crude residue was purified by flash chromatography (CH_2Cl_2/MeOH/NH_3 100:0.5:1) to afford the final compound **40** as a pale yellow solid (yield 17%). Rf: 0.39 (CH_2Cl_2/MeOH/NH_3 8.5:1.5:0.1); ^{1}H NMR (CD_3OD/$CDCl_3$) δ: 1.05 (dd, 3H, $J_1 = J_2 = 11.7$ Hz); 1.34 (s, 9H); 1.78–184 (m, 3H); 2.22–2.33 (m, 6H); 2.60 (bs, 1H); 3.27–3.33 (m, 4H); 3.41–3.53 (m, 8H); 7.00–7.05 (m, 4H); 7.21–7.27 (m, 4H); 7.38–7.50 (m, 6H); 7.57–7.63 (m, 2H); 7.99 (s, 2H). ESI-MS (m/z): 1006.6 [M + H$^+$].

*4.7. General procedure for N-Boc deprotection (**1**–**8**)*

N-Boc protected derivative (**33**–**40**, 0.03 mmol) was dissolved in CH_2Cl_2 (1 mL) and trifluoroacetic acid (1 mL) was added. The mixture was stirred at room temperature for 2 h and the reaction monitored by TLC (CH_2Cl_2/MeOH/NH_3 8.5:1.5:0.1). Then the solvent was removed under reduced pressure and the obtained salts (**1**–**8**) were characterized and utilized without any further purification.

*4.7.1. (Indole)$_2$-C$_2$-tach (**1**)*

Yield 80%; yellow solid; mp 229 °C; $R_f = 0.0$ (CH_2Cl_2/MeOH/NH_3 8.5:1.5:0.1); ν_{max} 3314–3095 (br), 1668, 1648, 1543, 1422, 1313, 1180, 1125; ^{1}H NMR (CD_3OD) δ: 1.53–1.70 (m, 3H); 2.41 (d, 1H, $J = 11.6$ Hz); 2.51 (d, 2H, $J = 11.6$ Hz); 3.26–3.52 (m, 5H); 3.65–3.75 (m, 2H); 7.04 (t, 1H, $J = 7.7$ Hz), 7.06 (s, 1H); 7.20 (t, 1H, $J = 7.7$ Hz); 7.26 (s, 1H); 7.37–7.44 (m, 3H); 7.60 (d, 1H, $J = 7.7$ Hz); 8.00 (s, 1H); ESI-MS (m/z): 474.1 [M + H$^+$]; HRMS (ESI): [M + H$^+$], found 474.2663. $C_{26}H_{32}N_7O_2$ requires 474.2617.

*4.7.2. (Indole)$_2$-C$_4$-tach (**2**)*

Yield 96%; yellow solid; mp 227 °C; $R_f = 0.0$ (CH_2Cl_2/MeOH/NH_3 8.5:1.5:0.1); ν_{max} 3360–3110 (br), 1669, 1630, 1546, 1421, 1313, 1181, 1115; ^{1}H NMR (CD_3OD) δ: 1.60 (dd, 3H, $J_1 = J_2 = 11.7$ Hz); 1.65–1.80 (m, 4H); 2.40 (d, 1H, $J = 11.7$ Hz); 2.49 (d, 2H, $J = 11.6$ Hz); 3.07–3.13 (m, 2H); 3.29–3.45 (m, 5H); 6.99–7.05 (m, 2H); 7.19 (t, 1H, $J = 7.8$ Hz); 7.25 (s, 1H); 7.37–7.45 (m, 3H); 7.59 (d, 1H, $J = 7.8$ Hz); 7.97 (s, 1H); ESI-MS (m/z): 502.3 [M + H$^+$]. HRMS (ESI): [M + H$^+$], found 502.2947. $C_{28}H_{36}N_7O_2$ requires 502.2930.

*4.7.3. (Indole)$_2$-C$_6$-tach (**3**)*

Yield 89%; white solid; mp 204 °C; $R_f = 0.0$ (CH_2Cl_2/MeOH/NH_3 8.5:1.5:0.1); ν_{max} 3316, 3305–3120 (br), 1669, 1635, 1548, 1418, 1311, 1180, 1125; ^{1}H NMR (CD_3OD) δ: 1.37–1.47 (m, 4H); 1.52–1.71 (m, 7H); 2.33–2.51 (m, 3H); 2.95–3.03 (m, 2H); 3.28–3.40 (m, 5H); 6.98–7.06 (m, 2H); 7.19 (t, 1H, $J = 7.6$ Hz); 7.25 (s, 1H); 7.36–7.44 (m, 3H); 7.60 (d, 1H, $J = 7.6$ Hz); 7.97 (s, 1H); ESI-MS (m/z): 530.2 [M + H$^+$]. HRMS (ESI): [M + H$^+$], found 530.3294. $C_{30}H_{40}N_7O_2$ requires 530.3243.

*4.7.4. (Indole)$_2$-C$_8$-tach (**4**)*

Yield 96%; white solid; mp 224 °C; $R_f = 0.0$ (CH_2Cl_2/MeOH/NH_3 8.5:1.5:0.1); ν_{max} 3350–3180 (br), 1668, 1633, 1544, 1420, 1310, 1179, 1125; ^{1}H NMR (CD_3OD) δ: 1.20–1.42 (m, 8H); 1.54–1.69 (m, 7H); 2.34–2.50 (m, 3H); 2.96–3.04 (m, 2H); 3.29–3.42 (m, 5H); 6.87 (s, 1H); 6.99–7.07 (m, 2H); 7.19 (t, 1H, $J = 7.8$ Hz); 7.26 (s, 1H); 7.37–7.44 (m, 2H); 7.60 (d, 1H, $J = 7.8$ Hz); 7.98 (s, 1H); ^{13}C NMR (CD_3OD) δ: 27.5 (t, 2C); 30.7 (t); 31.0 (t); 32.9 (t); 34.6 (t); 40.7 (t, 4C); 46.7 (t); 46.9 (d, 2C); 53.6 (d); 104.5 (d); 105.1 (d); 113.3 (d, 2C); 115.6 (d); 120.9 (d); 121.4 (d); 123.1 (d); 125.4 (d); 129.3 (s); 132.6 (s, 2C); 133.5 (s); 136.0 (s); 138.7 (s); 162.7 (s); 164.1 (s); ESI-MS (m/z): 558.3 [M + H$^+$]. HRMS (ESI): [M + H$^+$], found 558.3708. $C_{32}H_{44}N_7O_2$ requires 558.3556.

*4.7.5. Benzofuran-indole-C$_4$-tach (**5**)*

Yield 97%, dark yellow solid; mp 166 °C; $R_f = 0.0$ (CH_2Cl_2/MeOH/NH_3 8.5:1.5:0.1); ν_{max} 3220–3000 (br), 1668, 1628, 1557, 1446, 1259, 1178, 1126; ^{1}H NMR (CD_3OD) δ: 1.61 (dd, 3H, $J_1 = J_2 = 11.6$ Hz); 1.67–1.81 (m, 4H); 2.40 (d, 1H, $J = 11.6$ Hz); 2.51 (d, 2H, $J = 11.6$ Hz); 3.08–3.15 (m, 2H); 3.34–3.46 (m, 5H); 7.05 (s, 1H); 7.31 (t, 1H, $J = 7.7$ Hz); 7.41–7.57 (m, 3H); 7.58 (s, 1H); 7.62 (d, 1H, $J = 7.6$ Hz); 7.72 (d, 1H, $J = 7.7$ Hz); 8.04 (s, 1H); ^{13}C NMR (CD_3OD) δ: 24.8 (t); 28.0 (t); 34.6 (t); 39.6 (t, 3C); 46.3 (t); 47.0 (d, 2C); 53.6 (d); 104.7 (d, C_3); 112.0 (d); 113.3 (d, 2C); 115.8 (d); 121.0 (d); 124.0 (d); 125.2 (d); 128.1 (d); 129.1 (s); 131.8 (s, 2C); 133.4 (s); 136.2 (s); 156.8 (s); 159.6 (s); 163.5 (s); 164.4 (s); ESI-MS (m/z): 503.2 [M + H$^+$]. HRMS (ESI): [M + H$^+$], found 503.2819. $C_{28}H_{35}N_6O_3$ requires 503.2771.

*4.7.6. (Indole)$_2$-NH–CH$_2$–CH$_2$–O–CH$_2$–CH$_2$–NH-tach (**6**)*

Yield 92%; brown solid; $R_f = 0.0$ (CH_2Cl_2/MeOH/NH_3 8.5:1.5:0.1); ν_{max} 3305–3105 (br), 1670, 1629, 1546, 1434, 1312, 1180, 1124; ^{1}H NMR (CD_3OD) δ: 1.44 (dd, 3H, $J_1 = J_2 = 11.7$ Hz); 2.23 (d, 1H, $J = 11.7$ Hz); 2.41 (d, 2H, $J = 11.7$ Hz); 2.61–2.74 (m, 3H); 2.92–3.02 (m, 2H); 2.98–3.47 (m, 4H); 3.55–3.61 (m, 2H); 6.89 (t, 1H, $J = 7.9$ Hz); 6.93 (s, 1H), 7.04 (t, 1H, $J = 8.0$ Hz); 7.12 (s, 1H); 7.22–7.34 (m, 3H); 7.44 (d, 1H, $J = 7.9$ Hz); 7.83 (s, 1H); ^{13}C NMR (CD_3OD) δ: 40.2 (t); 43.6 (d, 2C); 46.0 (d, 2C); 46.9 (t, 2C); 50.0 (d); 66.9 (t); 71.6 (t); 104.8 (d); 105.1 (d); 113.1 (d); 113.4 (d); 115.7 (d); 121.1 (d); 121.3 (d); 122.9 (d); 125.3 (d); 129.2 (s); 132.4 (s, 2C); 133.4 (s); 136.0 (s); 138.6 (s); 160.8 (s); 162.7 (s); ESI-MS (m/z): 518.2 [M + H$^+$]. HRMS (ESI): [M + H$^+$], found 518.2893. $C_{28}H_{36}N_7O_3$ requires 518.2880.

*4.7.7. (Indole)$_2$-NH–(CH$_2$–CH$_2$–O)$_2$–CH$_2$–CH$_2$–NH-tach (**7**)*

Yield 94%; yellow solid; $R_f = 0.0$ (CH_2Cl_2/MeOH/NH_3 8.5:1.5:0.1);

ν_{max} 3325–3065 (br), 1671, 1615, 1547, 1436, 1312, 1180, 1124; ^{1}H NMR (CD_3OD) δ: 0.88 (dd, 3H, $J_1 = J_2 = 11.9$ Hz); 1.59 (dd, 3H, $J_1 = J_2 = 11.9$ Hz); 2.41–2.49 (m, 1H); 2.83–2.92 (m, 2H); 3.27–3.32 (m, 2H); 3.59–3.70 (m, 10H); 7.08 (t, 1H = J = 7.2 Hz); 7.1 (s, 1H); 7.24 (t, 1H, J = 7.3 Hz); 7.48 (s, 1H); 7.42–7.48 (m, 3H); 7.63 (d, 1H, J = 7.2 Hz); 8.02 (s, 1H); ESI-MS (m/z): 562.3 [M + H$^+$]. HRMS (ESI): [M + H$^+$], found 562.3128. $C_{30}H_{40}N_7O_4$ requires 562.3141.

*4.7.8. di-[(Indole)$_2$-NH–CH$_2$–CH$_2$–O–CH$_2$–CH$_2$–NH–]-tach (**8**)*

Yield 97%; orange solid; R_f = 0.0 (CH_2Cl_2/MeOH/NH_3 8.5:1.5:0.1); ν_{max} 3350–3085 (br), 1671, 1636, 1545, 1416, 1310, 1177, 1124; ^{1}H NMR (CD_3OD) δ: 0.89 (dd, 3H, $J_1 = J_2 = 10.6$ Hz); 1.61–1.67 (m, 3H); 2.48–2.56 (m, 2H); 2.81–2.89 (m, 8H); 3.50–3.62 (m, 9H); 7.02–7.09 (m, 4H); 7.21-7.29 (m, 4H); 7.39–7.48 (m, 6H); 7.58–7.64 (m, 2H); 8.01 (s, 2H); ^{13}C NMR (CD_3OD) δ: 40.1 (t); 43.6 (d, 2C); 45.9 (d, 2C); 46.9 (t, 2C); 50.0 (d); 66.9 (t); 71.6 (t); 104.9 (d, 2); 105.1 (d, 2C); 113.1 (d, 2C); 113.3 (d, 2C); 115.7 (d, 2C); 121.1 (d, 2C); 121.3 (d, 2C); 122.9 (d, 2C); 125.3 (d, 2C); 129.2 (s, 4C); 132.4 (s, 4C); 133.1 (s, 2C); 136.0 (s, 2C); 138.6 (s, 2C); 162.6 (s); 162.9 (s); ESI-MS (m/z): 944.9 [M + K$^+$]. HRMS (ESI): [M + H$^+$], found 906.4589. $C_{50}H_{56}N_{11}O_6$ requires 906.4415.

4.8. Electrophoretic procedure for DNA binding/cleavage experiments

Stock solutions of the tach minor groove binders conjugates **1**–**8** and tach (0.5–1 mmol) were prepared in H_2O/CH_3OH 2:1 (ligands **1**–**3**, **5**–**8**) and H_2O/CH_3OH 2:3 (ligand **4**). The ligand was diluted in the proper solvent mixture, one equivalent of $Zn(NO_3)_2$ or $Cu(NO_3)_2$ in water was added and the pH was corrected to 7 by addition of NaOH. The methanol content in the final reaction mixtures was always lower than 4%. DNA cleavage experiments were performed using pBR 322 (Gibco BRL) in 20 mM HEPES, pH 7.1. Reactions were performed by incubating DNA (12 μM base pairs) at 37 °C in the presence/absence of increasing amounts of metal complex for the indicated time. Reaction products were resolved on a 1% agarose gel in TAE buffer (40 mM TRIS base, 20 mM, acetic acid, 1 mM EDTA) containing 1% SDS to dissociate the ligands from DNA. The resolved bands were visualized by ethidium bromide staining and photographed. The relative amounts of different plasmid structures were quantified using a BioRad Gel Doc 1000 apparatus interfaced to a PC workstation. DNA binding experiments were performed as reported in the previous paragraph but the reaction mixture was loaded immediately on the agarose gel without incubation time and the TAE buffer did not contain EDTA and SDS.

4.9. UV-VIS titrations

Spectrophotometric titrations were performed with a Perkin-Elmer λ20 in 20 mM HEPES, pH 7.1. Binding was followed by addition of increasing amounts of ctDNA to a freshly prepared ligand solution in 20 mM HEPES, pH 7.1. Experimental data were analyzed in terms of relative variation of the absorbance as a function of DNA concentration.

4.10. CD measurements

Circular dichroism spectra were recorded at 25 °C using 1 cm path length quartz cells on a Jasco J 810 spectropolarimeter equipped with a NESLAB temperature controller. CD spectra were recorded on samples containing 80 μM ctDNA and 40 ligands concentrations in 20 mM HEPES, pH 7.1. The reported spectrum of each sample represents the average of 3 scans. Observed ellipticities were converted to mean residue ellipticity [θ] = deg x cm^2 x dmol^{-1} (Mol. Ellip.).

4.11. Molecular modeling studies

Zn(II)-tach complexes were optimized using Hartree-Fock calculations with the 6–311++G(d,p) basis set. A water molecule coordinated to the apical position of Zn metal ion was used. This water molecule was used to saturate, at least partially, the coordination sphere of the zinc metal ion. Quantum chemistry calculations were carried out with *Gaussian 03*.[33] Harmonic vibrational frequencies were obtained from RHF/6–311++G(d,p) calculations and used to characterize local energy minima (all frequency real). Atomic charges were calculated by fitting to electrostatic potential maps (CHELPG method). Structures of metal complex- conjugates were built using the "Builder" module of Molecular Operation Environment (MOE, version 2013.08).[34] Conjugates complexes were minimized using MMFF94 force field. All bond distances involving Zn(II) metal ion are freeze during the optimization step. Charges for the Zn(II)-triaminocyclohexane complexes were imported from the Gaussian output files.

The present study involved the use of consensus dinucleotide intercalation geometries d(ApT) and d(GpC) initially obtained using NAMOT2 (Nucleic Acid MOdeling Tool, Los Alamos National Laboratory, Los Alamos New Mexico), software.[35] d(ApT) and d(GpC) intercalation sites were contained in the centre of a decanucleotide duplex of sequences d(5′-ATATA-3′)$_2$ and d(5′-GCGCG-3′)$_2$ respectively. Decamers in B-form were built using the "DNA Builder" module of MOE. Decanucleotides were minimized using Amber94 all-atom force field,[36] implemented by MOE modeling package, until the *rms* value of Truncated Newton method (TN) was <0.001 kcal mol^{-1} Å^{-1}. The dielectric constant was assumed to be distance independent with a magnitude of 4. The metal complex-minor groove binder conjugates (**3** and **8**) were docked into both intercalation sites using flexible MOE-Dock methodology. The purpose of MOE-Dock is to search for favorable binding configurations between a small, flexible ligand and a rigid macromolecular target. Searching is conducted within a user-specified 3D docking box, using "tabù search" protocol[37] and MMFF94 force field.[38] MOE-Dock performs a user-specified number of independent docking runs (55 in our specific case) and writes the resulting conformations and their energies to a molecular database file. The resulting DNA-minor groove binder complexes were subjected to MMFF94 all-atom energy minimization until the *rms* of conjugate gradient was <0.1 kcal mol^{-1} Å^{-1}. Also in these step, all bond distances involving Zn(II) metal ion are freeze during the energy optimization. To model the effects of solvent more directly, a set of electrostatic interaction corrections are used. MOE suite implemented a modified version of GB/SA contact function described by Still and co-authors.[39] These terms model the electrostatic contribution to the free energy of solvation in a continuum solvent model. The interaction energy values were calculated as the energy of the complex minus the energy of the ligand, minus the energy of DNA: $DE_{inter} = E_{(complex)} - (E_{(L)} + E_{(rDNA)})$.

Acknowledgments

The authors thank dr. Tiziana De Luca and dr. Silvia Masetto for their involvement in synthetic work. This work was supported by Fondazione Beneficentia Stiftung, MIUR-PRIN 2010JMAZML and UNITS-FRA_2015 projects. The molecular modeling work coordinated by S.M. has been carried out with financial support from the University of Padova, Italy, and from the MIUR, PRIN 2010–2011, 20103W4779_004 project. S.M. is also very grateful to Chemical Computing Group for the scientific and technical partnership.

References

1. Basile LA, Raphael AL, Barton JK. *J Am Chem Soc*. 1987;109:7550–7551.
2. Mancin F, Scrimin P, Tecilla P. *Chem Commun*. 2012;48:5545–5559.
3. Aiba Y, Sumaoka J, Komiyama M. *Chem Soc Rev*. 2011;40:5657–5668.
4. Wende C, Lüdtke C, Kulak N. *Eur J Inorg Chem*. 2014:2597–2612.
5. Mancin F, Tecilla P. *New J Chem*. 2007;31:800–817.
6. Liu C, Wang L. *Dalton Trans*. 2009:227–239.
7. Brown RS, Lu Z-L, Liu CT, Tsang WY, Edwards DR, Neverov A. *J Phys Org Chem*. 2010;23:1–15.
8. Boseggia E, Gatos M, Lucatello L, et al. *J Am Chem Soc*. 2004;126:4543–4549.
9. Krauser JA, Joshi AL, Kady IO. *J Inorg Biochem*. 2010;104:877–884.
10. Tseng T-SA, Burstyn JN. *Chem Commun*. 2008:6209–6211.
11. Sissi C, Rossi P, Felluga F, et al. *J Am Chem Soc*. 2001;123:3169–3170.
12. Chen X, Fan J, Peng X, et al. *Bioorg Med Chem Lett*. 2009;19:4139–4142.
13. Copeland KD, Fitzsimons MP, Houser RP, Barton JK. *Biochemistry*. 2002;41:343–356.
14. Xia C-Q, Jiang N, Zhang J, et al. *Bioorg Med Chem*. 2006;14:5756–5764.
15. Wang J-T, Xia Q, Zheng X-H, et al. *Dalton Trans*. 2010;39:2128–2136.
16. Lönnberg T, Aiba Y, Hamano Y, Miyajima Y, Sumaoka J, Komiyama M. *Chem Eur J*. 2010;16:855–859.
17. Zelder FH, Mokhir AA, Krämer R. *Inorg Chem*. 2003;42:8618–8620.
18. Hettich R, Schneider HJ. *J Am Chem Soc*. 1997;119:5638–5647.
19. An Y, Lin YY, Wang H, et al. *J Chem Soc Dalton Trans*. 2007:1250–1254.
20. Geierstanger BH, Mrksich M, Dervan PN, Wemmer DE. *Science*. 1994;266:646–650.
21. Kielkopf CL, Baird EE, Dervan PB, Rees DC. *Nat Struct Biol*. 1998;5:104–109.
22. Boger DL, Johnson DS. *Angew Chem Ed Engl*. 1996;35:1438–1474.
23. Trauger JW, Baird EE, Dervan PB. *J Am Chem Soc*. 1998;120:3534–3535.
24. Boger DL, Johnson DS. *Proc Natl Acad Sci U. S. A*. 1995;92:3642–3649.
25. Li C, Qiao R-Z, Wang Y-Q, Zhao Y-F, Zeng R. *Bioorg Med Chem Lett*. 2008;18:5766–5770.
26. Li C, Du C, Tian H, et al. *Chem Eur J*. 2010;16:12935–12940.
27. Rossi P, Tecilla P, Baltzer L, Scrimin P. *Chem Eur J*. 2004;10:4163–4170.
28. Boger DL, Yun W, Han N. *Bioorg Med Chem*. 1995;3:1429–1453.
29. Itoh T, Hisada H, Sumiya T, Hosono M, Usui Y, Fujii Y. *Chem Commun*. 1997:677–678.
30. Keller M, Jorgensen MR, Perouzel E, Miller AD. *Biochemistry*. 2003;42:6067–6077.
31. Yu Z, Schmaltz RM, Bozeman TC, et al. *J Am Chem Soc*. 2013;135:2883–2886.
32. Sato H, Hayashi E, Yamada N, Yatagai M, Takahara Y. *Bioconj Chem*. 2001;12:701–710.
33. Frisch MJ, Trucks GW, Schlegel HB, et al. *Gaussian 03, Revision C.02*. Wallingford CT: Gaussian, Inc.; 2004.
34. *Molecular Operating Environment (MOE), 2013.08*. 1010 Sherbooke St. West, Suite #910, Montreal, QC, Canada, H3A 2R7: Chemical Computing Group Inc.; 2015.
35. NAMOT2 (Nucleic Acid MOdeling Tool), Los Alamos National Laboratory, Los Alamos New Mexico.
36. Cornell WD, Cieplak WP, Bayly CI, et al. *J Am Chem Soc*. 1995;117:5179–5197.
37. Baxter CA, Murray CW, Clark DE, Westhead DR, Eldridge MD. *Proteins Struct Funct Genet*. 1998;33:367–382.
38. Halgren TA. *J Comput Chem*. 1996;17:490–519.
39. Qiu D, Shenkin S, Hollinger FP, Still WC. *J Phys Chem*. 1997;101:3005–3014.